applied sciences

MDPI

Article

Study on Mechanism of Stick–Slip Vibration Based on Torque Characteristics of PDC Bit

Lijun Li [1], Chunliang Zhang [2,*] and Aixuan Wu [2]

[1] Dean's Office of Nanchong Campus, Southwest Petroleum University, Nanchong 637001, China; cindy_1004888@163.com
[2] Department of Mechanical Engineering, School of Mechanical and Electrical Engineering, Southwest Petroleum University, Chengdu 610500, China; 15330721459@163.com
* Correspondence: zhangchunliang6666@163.com

Abstract: Stick–slip vibration (SV) of drill string systems is the main cause of fatigue failure of PDC bits under complex drilling conditions. Exploring its mechanism is helpful for identifying the causes of bit failure and developing preventive measures to prolong bit service life. In this study, the influence of various factors on torque characteristics is tested by drilling rock breaking with various PDC bits and the variations in torsion variables and torsion speed of drill string systems under different torque loading conditions of drill bits are ascertained. Through a finite element simulation of the drill string–bit system, the influence of the PDC bit on the torsional deformation with variable torque is determined, and the influence mechanisms of bit size, tooth structure, invasion depth, rock strength, and other factors on the SV induced by a PDC bit are established. The results show that the change in the reaction resistance moment of the formation rock leads to variation in the driving speed of the drill string system, which is one of the main reasons for the SV. Even if the torque change in the bit is minor, SV will occur if the drill string is too long.

Keywords: PDC bit; stick–slip vibration; string mechanics; torque characteristic; failure

Citation: Li, L.; Zhang, C.; Wu, A. Study on Mechanism of Stick–Slip Vibration Based on Torque Characteristics of PDC Bit. *Appl. Sci.* **2024**, *14*, 6419. https://doi.org/10.3390/app14156419

Academic Editor: Marco Troncossi

Received: 7 May 2024
Revised: 14 July 2024
Accepted: 15 July 2024
Published: 23 July 2024

1. Introduction

Polycrystalline diamond compact (PDC) drill bits are a type of drilling equipment used in the oil and gas industry. These drill bits are equipped with synthetic diamond cutters that have been carefully engineered to provide superior strength and wear resistance. When a PDC bit is drilling in gravel-bearing stratum, soft-hard alternating stratum, directional drilling, and other complex working conditions lead to impact loads. These impact loads mainly originate from longitudinal, transverse, and torsional vibration of the drill string system. In particular, the impact load introduced by longitudinal vibration can impose an impact force of up to several tons on the cutting teeth. SV is the most dangerous, facilitating the transition of the cutting teeth into a reverse cutting motion. The impact load often encountered leads to abnormal fatigue failure accidents such as cutting teeth breaking, delamination, and tooth breaking, all of which dramatically reduce the service life and drilling efficiency of the bit [1–4]. Moreover, SV of the drill string system is the main cause of PDC bit fatigue failure [5–7]. The causes of SV include cementation of cuttings and blockage of a heterogeneous formation, change in lithology, transverse vibration in compound drilling, etc. [8–11]. When a PDC bit produces SV, this will aggravate abnormal fatigue damage of the bit, which will reduce rock-breaking energy during its service life, resulting in a decrease in drilling efficiency and possible wellbore safety risks [12–17]. Therefore, research on the torque characteristics of PDC bits to reveal the mechanism of SV is very important for the technical means and application technology to suppress SV and improve drilling efficiency and safety.

Vaziri et al., Cruz Neto et al., and Ulf et al. [18–20] studied the causes and formation mechanism of SV and put forward a technical means to eliminate drill string vibration

through the bottom hole assembly. Bi Siyi, and Selnes et al. [21,22] proposed a PDC bit penetration depth adjustment control technology as a control for bit SV suppression. Implementation of this technology significantly improved the antivibration performance of the bit. Bakhtiari-Nejad and Hosseinzadeh, Chen et al., and Thomas et al. [23–25] used bit vibration sensors to identify the SV characteristics of PDC bits caused by cutting and proposed a control to reduce SV by optimizing drilling parameters. Boukredera et al. [26] studied the influence of cutting depth per tooth and rock drillability on SV of PDC bits through indoor dynamic rock-breaking experiments. Paulin et al., Lobo et al., Caresta, and Kapitaniak et al. [27–30] examines the effectiveness of active control of the braking coefficient, using an On–Off-based control scheme with proportional control. The results show that active control can improve the drill string behavior both when drilling and when rotating off-bottom by reducing the slippage of the sleeves. Guo et al., Real et al., Richard et al., Besselink et al., and Silveira et al. [31–35] established a longitudinal–transverse–torsional coupling vibration model and SV characteristics of drill strings in ultra-high-temperature and high-pressure curved wells. The influence of rotary table speed, weight on bit (WOB), torsion punch speed-up tools, and bottom hole assembly length on SV characteristics of drill string systems was explored. Mendil et al., Jain et al., Yang et al., Thorsten et al., and Hareland et al. [36–40] conducted research on rock-breaking mechanisms and drilling rock breaking of separated impact-scraping composite bits that has important reference value for the development and application of new impact-scraping composite PDC bits.

The penetration depth of PDC bits with different structures during drilling is crucial to the load on the drill string system. Most of the research work described above focuses on the system dynamics behavior of the "drill string–drill bit–rock" system. However, due to the instantaneous change in the penetration depth of the drill bit, the resulting sudden change in torque load will inevitably have a significant impact on inducing stick–slip vibration in the drill string system.

2. Working Torque Characteristics of PDC Bit Drilling

In this section, the influence of the diameter of the PDC bit tooth arrangement and the penetration depth on the working torque of the PDC bit is addressed, and the mechanism of SV phenomenon is described. Nine kinds of tooth density, three bit diameters, seven groups of intrusion depths, and five groups of typical rocks were selected, as listed in Tables 1 and 2.

Table 1. Structural features and dimensions of PDC bits.

Bit Serial Number	Model	Number of Cutting Teeth	Diameter of Cutting Teeth, mm	Remarks
#1	8½″ 604	19	19	4-blade, sparse tooth distribution
#2	8½″ 605	22	19	5-blade, sparse tooth distribution teeth
#3	8½″ 505	25	16	5-blade, low-densely distributed teeth
#4	8½″ 506	28	16	6-blade, low-densely distributed teeth
#5	8½″ 406	31	13	6-blade, medium-densely distributed teeth
#6	8½″ 407	34	13	7-blade, medium-densely distributed teeth
#7	8½″ 408	41	13	8-blade, highly densely distributed teeth
#8	6″ 406	28	13	Smaller diameter size
#9	12¼″ 606	43	19	Smaller diameter size

Table 2. Strength condition of formation rock.

Type of Rock Block	Lanea50	Mimosa70	Baobab100	Mimosa130	Mimosa170
Compressive strength (MPa)	51	75	106	133	175
Rock strength category	Softer	Medium softness	Hard	Medium hardness	High hardness

3. Materials and Methods

The structures of these above nine types of PDC bits are shown in Figure 1, where #1 to #7 are 8½″ bits, bit #8 is a 6″ bit, and bit #9 is a 12¼″ bit.

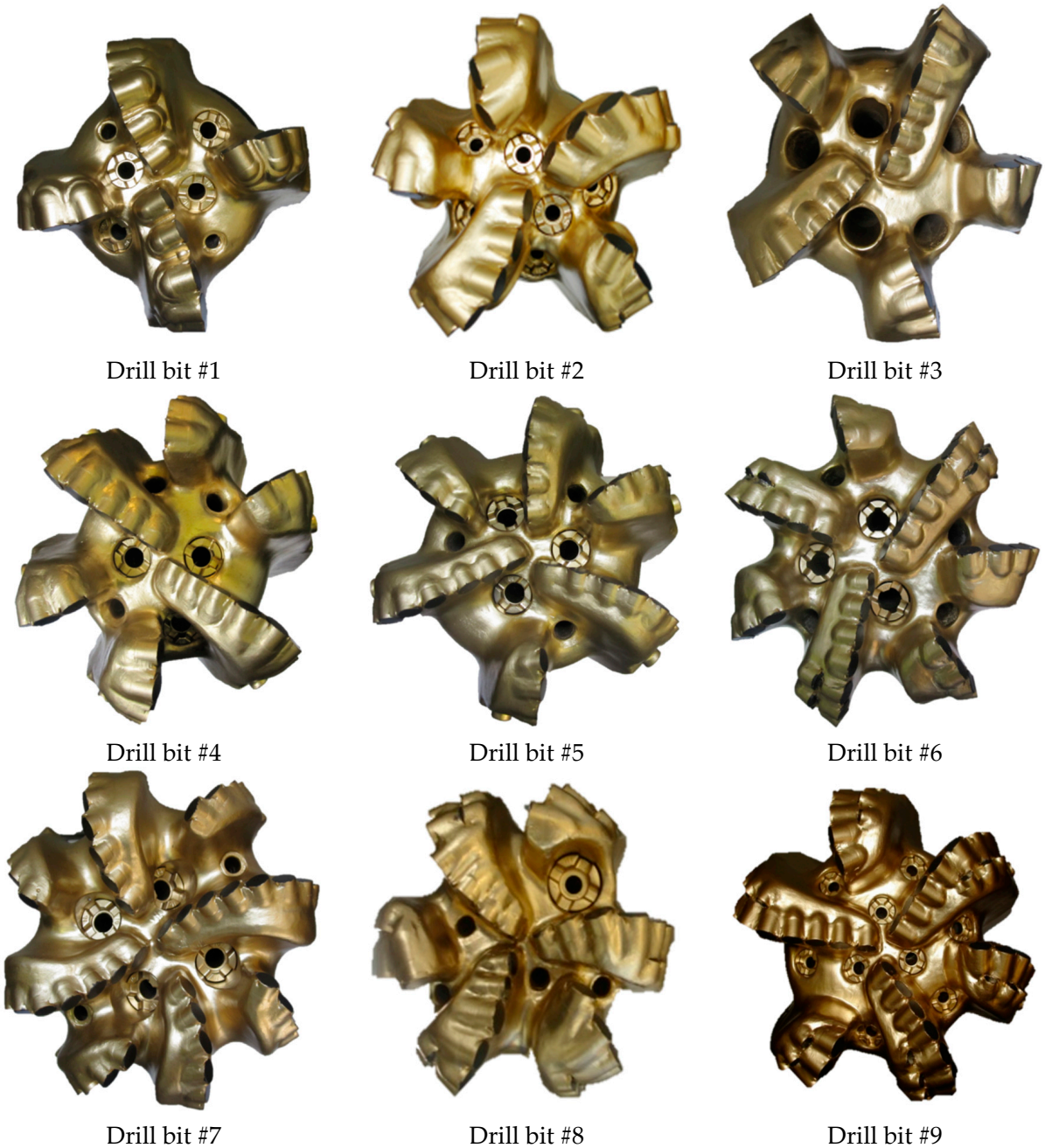

Figure 1. Nine kinds of PDC bits with different tooth densities and different sizes.

Drilling experiments were conducted on a 300 kN full-scale bit test bench with the above nine bits, and the rotating speed was set to 60 rpm. By applying WOB, the drilling bit working torque, penetration rate, and other parameters were analyzed, respectively. The intrusion depth of the bit under each experimental condition was converted according to the intrusion rate and rotating speed parameters, thus forming a characteristic intrusion depth versus torque relationship. The experimental equipment and the bottom hole formed by drilling are shown in Figure 2.

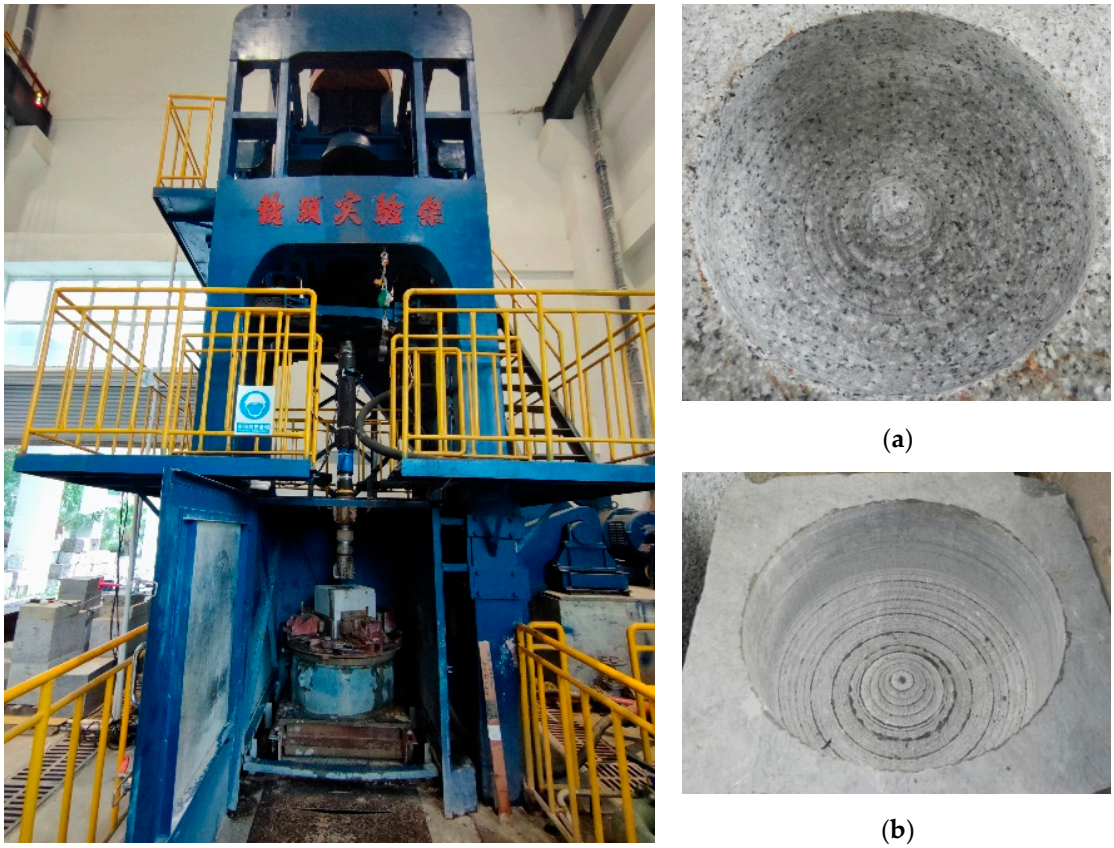

(**a**)

(**b**)

Figure 2. Full bit drilling experimental and bottom holes. (**a**) Mimosa170 block bottom hole; (**b**) Baobab100 block bottom hole.

3.1. Influence of the Cutting Structure

According to the above experimental results, the tooth distribution density of seven kinds of 8½″ PDC bits is gradual and the strength of rock blocks in five strata gradually increased. The "penetration depth–torque" relationship characteristic is shown in Figure 3.

It can be seen from the figure that the working torque of the PDC bit has little influence on parameters such as tooth distribution density and blade number, and the torque difference of various types of bits is <7% under the same invasion depth. The characteristic intrusion depth–torque curves in rocks of different strengths increase linearly, but with the increase in rock strength, they exhibit a positive correlation trend, demonstrating that rock strength has a significant influence on the torque characteristics of PDC bit drilling.

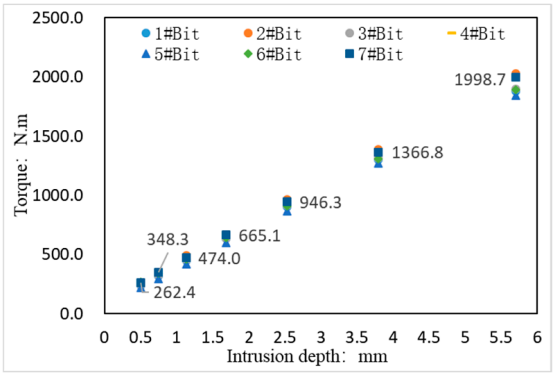

(**a**)

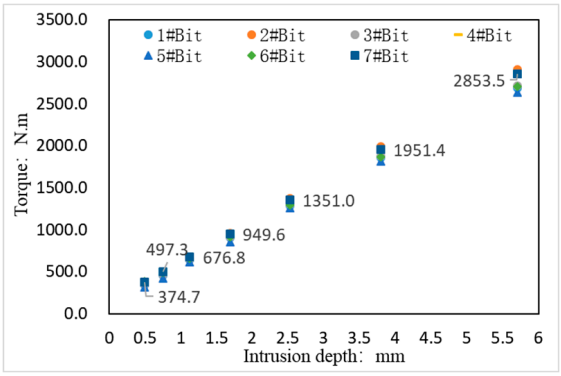

(**b**)

Figure 3. *Cont.*

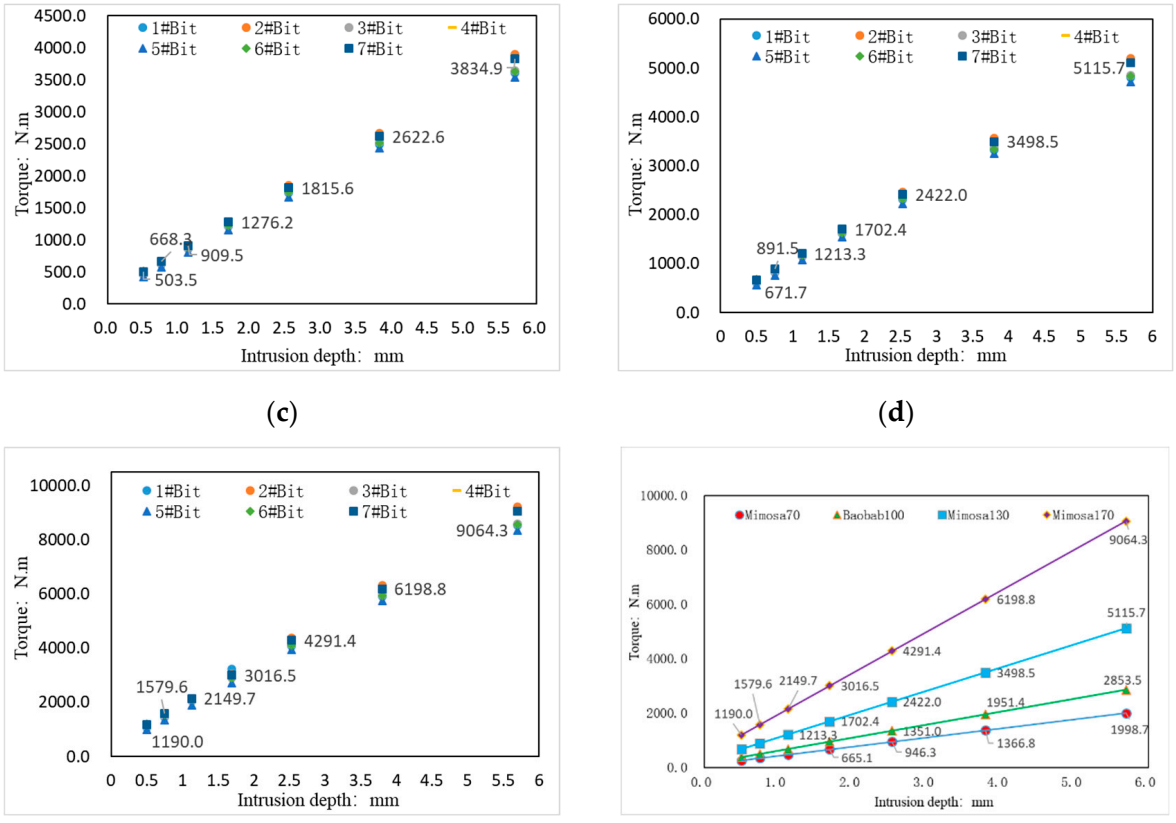

(**c**) (**d**)

(**e**) (**f**)

Figure 3. Comparison of penetration depth and torque for seven types of PDC bits. (**a**) Lanea50 rock block; (**b**) Mimosa70 rock block; (**c**) Baobab100 rock block; (**d**) Mimosa130 rock block; (**e**) Mimosa170 rock block; (**f**) Transverse comparison of bit torque characteristics.

3.2. Influence Relationship of Bit Size

Experiments with PDC bits of different sizes (6″, 8½″ and 12¼″, respectively) were conducted. The characteristics of the invasion depth–torque relationship are shown in Figure 4. The strength of rock blocks in five strata gradually increases.

It can be seen from the figure that the bit size has an obvious influence on the working torque of the PDC bit. The greater the size of the bit, the greater the torque value under the same intrusion depth. These factors will have a significant influence on the occurrence of SV and impact dynamic load of the bit.

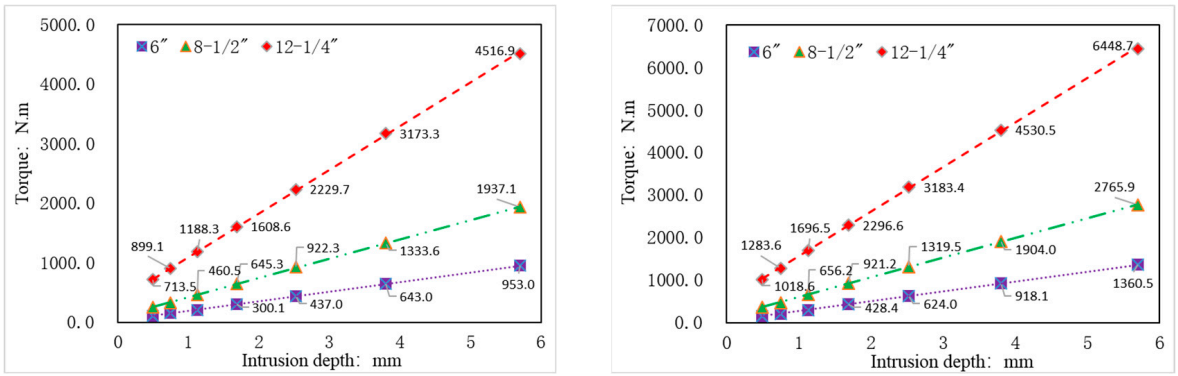

(**a**) (**b**)

Figure 4. *Cont.*

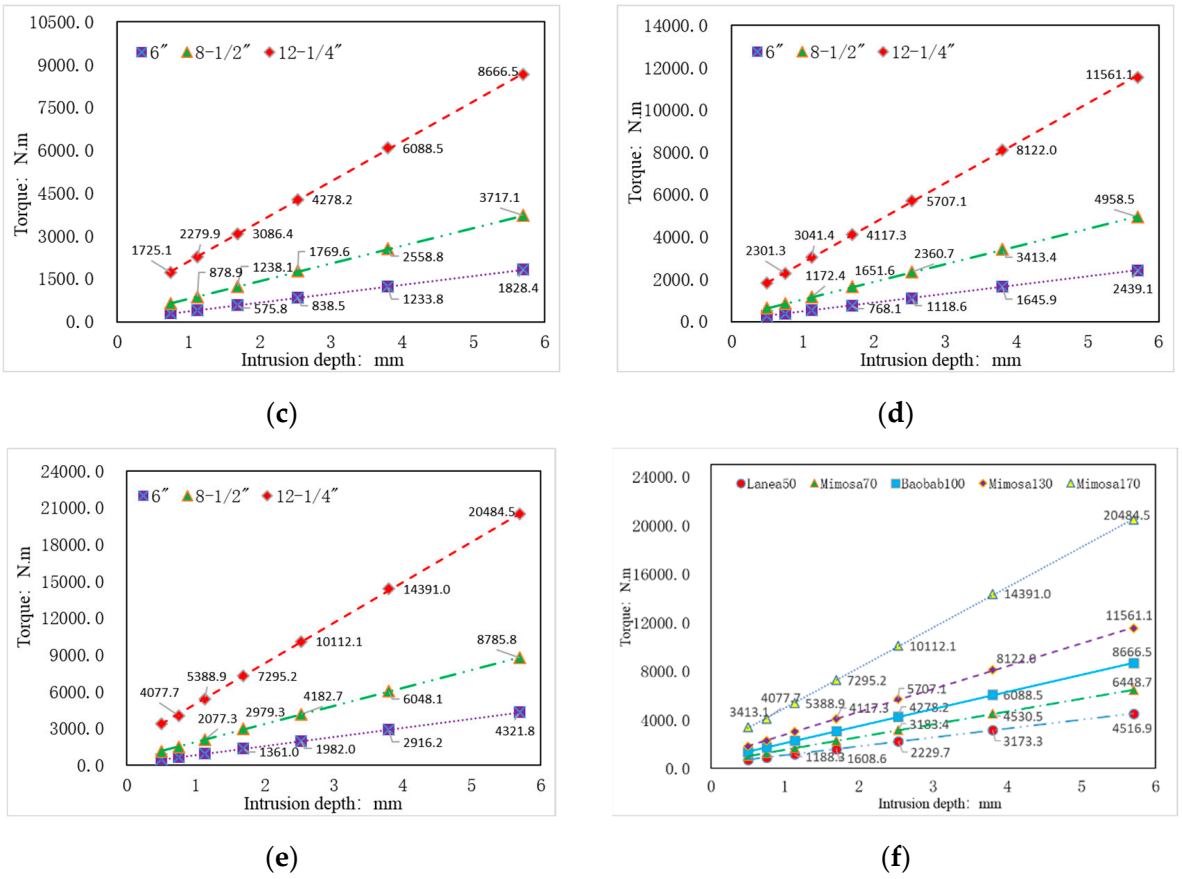

Figure 4. Comparison of "penetration depth–torque" characteristic relationship curves of PDC bits of three different sizes. (**a**) Lanea50 rock block; (**b**) Mimosa70 rock block; (**c**) Baobab100 rock block; (**d**) Mimosa130 rock block; (**e**) Mimosa170 rock block; (**f**) 12¼″ transverse comparison of bit torque characteristics.

4. Study on Torsion Variable Characteristics of PDC Bit Drilling Drill String

The fundamental reason for SV of PDC bits is that the fluctuation of bit working torque leads to the instantaneous change in the bit rotating speed. With the rotation of the drill string system, this energy is stored in the form of elastic deformation. When this deformation reaches a certain degree, it is enough to overcome the rotation retardation of the rock on the bit, and this energy will be released instantaneously in the form of a cycle of SV. Therefore, the torsion variable of the drill string system is important in the relationship between torque and speed. A structural schematic diagram of the rock–bit–drill string system is shown in Figure 5.

The formula of the drill pipe rotation variable in the above figure is shown below:

$$\varphi = \frac{Tl}{GI_p}$$

$I_p = \frac{\pi D^4}{32}(1-\alpha^4)$—Cross-sectional moment of inertia;
$\alpha = D/d$;
T—Working torque of drill bit;
L—Drill pipe length;
$G = \frac{E}{2(1+\varepsilon)}$—Shear modulus;
E—Elastic modulus;
ε—Poisson's ratio.

According to industry standards (SY/T 5561) [41], the elastic modulus of drill pipe material corresponding to G-grade reinforced steel pipe material has a Poisson ratio of 0.3. The length of the drill pipe was set to 1000 m according to the specific working condition, and the torsion variables were, respectively, determined according to the three bit sizes used in the five strata and rocks.

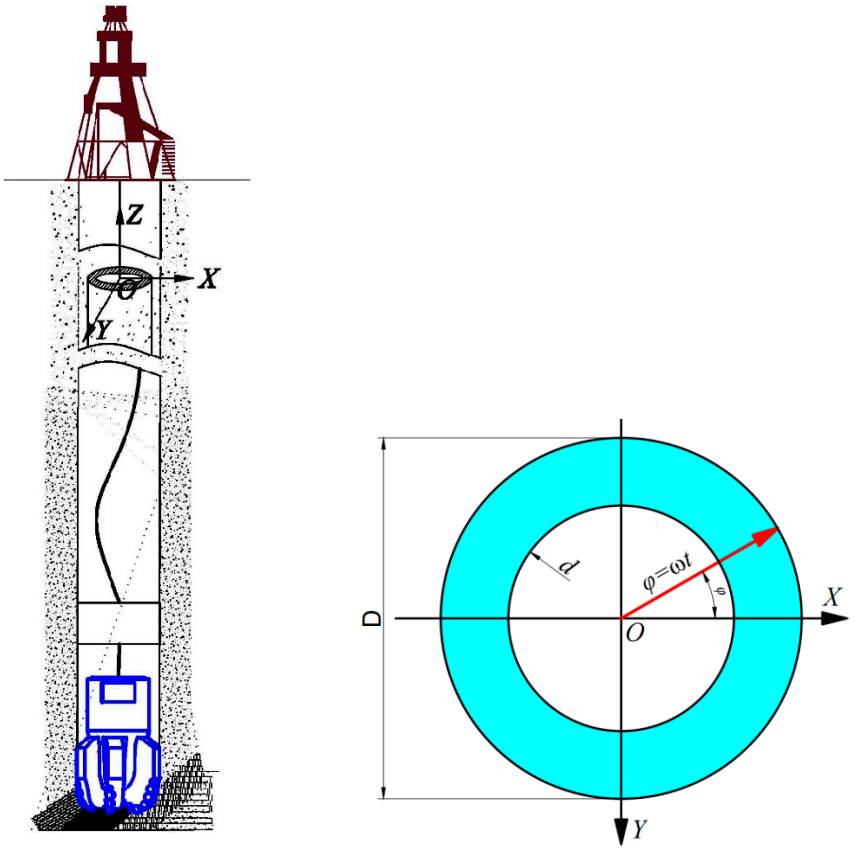

Figure 5. Schematic diagram of the drill string torsion variable.

The material properties of drill string steel pipe are listed in Table 3.

Table 3. Material properties of the drill string steel pipe.

Bit Size /in	Outer Diameter /in	Inner Diameter /in	Wall Thickness /mm	Shear Modulus /Pa	Cross-Sectional Moment of Inertia / m^4
6″	3-1/2″	2-3/4″	9.35	7.92×10^{10}	1.871×10^{-5}
8-1/2″ 12-1/4″	5″	4-1/4″	9.19		5.94×10^{-5}

4.1. Relationships among Drill String Torsion Variables

The penetration depths of medium and fine bits are as follows: 0.25, 0.50, 0.75, 1.00, 1.25, 1.50, 2.00, 2.50, and 3.00 mm. The relationship between drill string torsion variables is shown in Figure 6.

It can be seen from the figure that the most obvious torsion variable is that of the 12¼″ bit, followed by 6″ and 8½″ bits after the penetration depth of PDC bit changes. In particular, the torsional variation of the 12¼″ bit in the Minmosa 170 (compressive strength = 175 MPa) rock block reaches 443.85° (1.23 cycles) when the penetration depth reaches 3 mm.

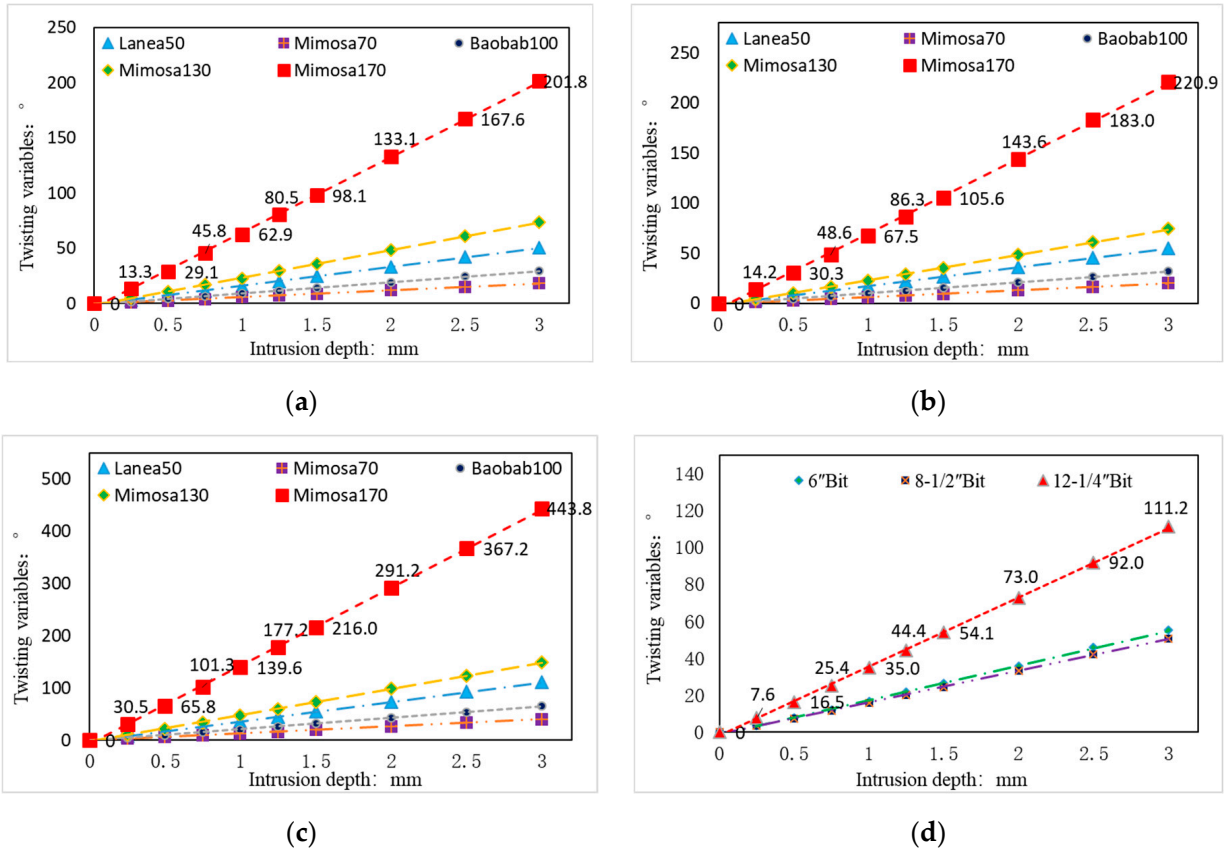

Figure 6. Comparison between invasion depth and the torsion variable of PDC bits of three sizes. (**a**) 6″drill bit; (**b**) 8½″ drill bit; (**c**) 12 ¼″ drill bit; (**d**) Comparison of torsion variables of three bits (Lanea50).

4.2. Torsion Velocity Change in the Drill String

When the formation lithology of the PDC bit changes suddenly, its rotational speed will change significantly through the torsion variable The influence of penetration depth on bit speed is shown in Figure 7, wherein the marked speed change is the relative change.

We can consider the 1000 m-long drill pipe as an example and assume a rotational speed of 80 rpm (the red dotted line position marked in the figure). The overall trend of the 6″ PDC bit increases with the strength of the formation rock. When drilling in the Mimosa170 rock block, the bit speed can be reduced from 80 to 73 rpm with a variation of 3 mm intrusion depth per unit time. This is the deceleration state and then returns to 80 rpm. This shows that the change in penetration depth (or the sudden change in WOB) has a significant influence on the bit speed.

Taking the 8½″ PDC bit as an example, we see that this type of bit has the least influence on the speed fluctuation owing to the change in penetration depth compared with that of the 6″ and 12¼″ bits. A longitudinal comparison of different lithologic changes, such as an intrusion depth of 1 mm, from the Lanea50 formation block to the Mimosa170 formation block reveals that the change in rotational speed per unit time is 2.14 rpm.

For the 12¼″ PDC bit, in the Mimosa130 formation rock block, when the initial state of the bit is at a high invasion depth (e.g., 3.0 mm) and drops to 0.25 mm per unit time, the resistance torque of the rock suddenly decreases, and the accumulated torsion variable in the drill string system is released to the bit to accelerate its speed to be >80 rpm (increasing to 82.59 rpm). This is an accelerated state.

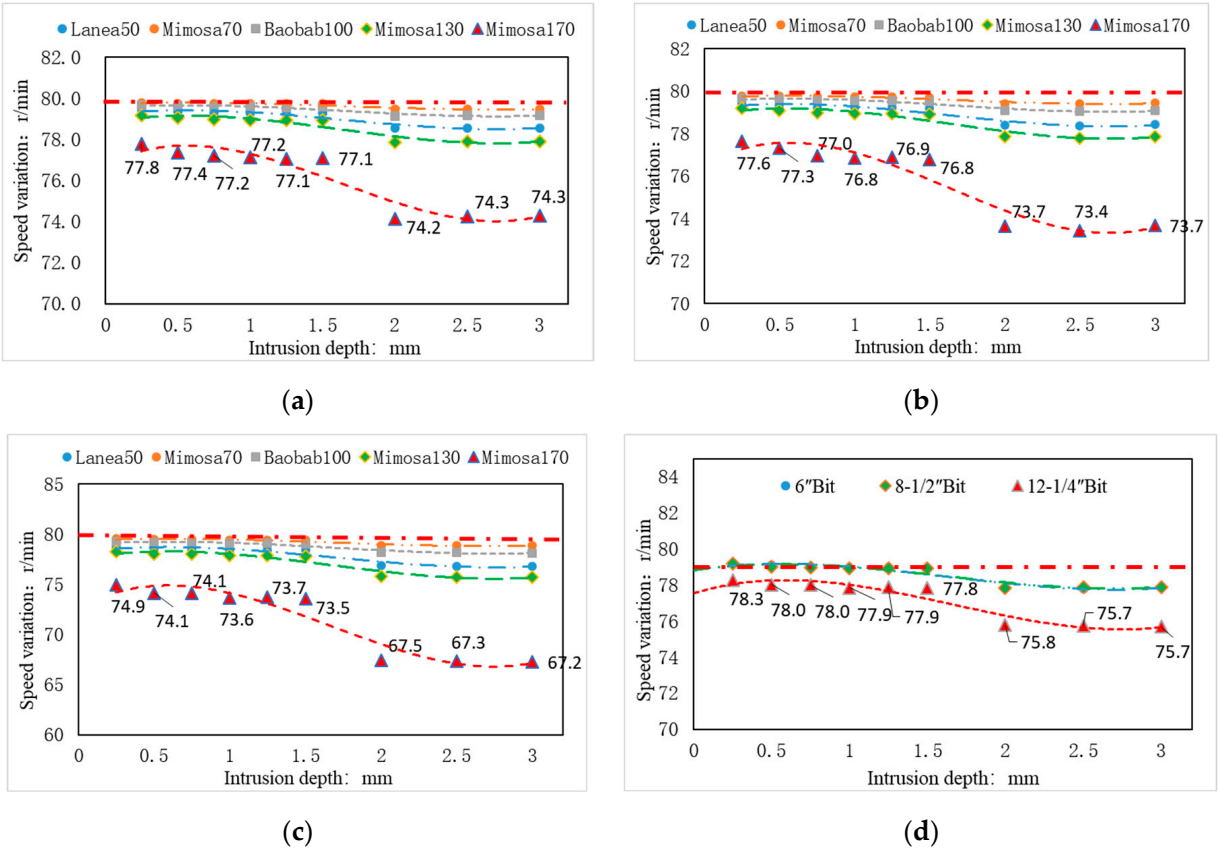

Figure 7. Comparisons between penetration depth and torsion speed of PDC bits of three sizes. (**a**) 6″drill bit; (**b**) 8½″ drill bit; (**c**) 12¼″ drill bit; (**d**) Comparison of rotational speed changes of three bits (Mimosa130).

5. Mechanism of SV of PDC Bit in Drilling

5.1. Simulation of Torsion of the Bit–Drill String System

SV of the bit appears alternately as evident by bit viscosity and slippage. In the viscous stage, the drill bit decelerates and rotates while the drill string system continues to rotate under the drive of the turntable, resulting in distortion. The most direct manifestation of the accumulated energy of the drill string is the rapid torque load. In the slippage stage, when the torque buildup at the tip–rock contact becomes enough to drive the bit to break, the drill string energy instantly releases the forward rotation of the bit and suddenly accelerates the bit penetration rate several times faster than the rotating speed and torque of the rotary table. Figure 8 shows a schematic diagram of SV of the bit, in which the bit speed is the rotary table speed.

When SV occurs, the torque and speed near the bit become lower in the SS stage, and the torque becomes lower and the speed becomes higher in the slippage stage until a dynamic balance is reached. To describe this phenomenon, a finite element simulation was performed by establishing a drill string–bit system. The total length of the drill string was set to 3000 m, and the diameter was set to 5″ (φ127 mm). PIPE31 drill pipe was adopted as the unit type. The specific parameters are listed in Table 4.

Figure 9 shows the structure of the drill string system. Figure 10 shows that the total number of unit nodes was 300 per 10 points and one meter of unit nodes. In the simulation, the rotary table was given a constant speed of 80 rpm, the simulation time was 40 s, and a variable torque load was applied to the bit.

In the simulation, the torque applied to the bit (static loading) decreases the angular velocity while the rotating speed of the rotary table remains unchanged. Figures 11 and 12 show the torque and stress distribution, respectively, of the drill string at a simulation time

of 34 s in which the bit torque had a rectangular wave load amplitude (dynamic loading). When the simulation time reached 22.1 s, the peak torque increases. The torque of the drill string decreases gradually from the wellhead to the bottom hole, and distortion always occurs. Therefore, the torsion variable at the turntable is larger and the accumulated energy is higher. Because the torsion variable at the wellhead is much larger than that at the bottom of the well, greater stress will be produced at the wellhead, which will cause early failure of the drill pipe.

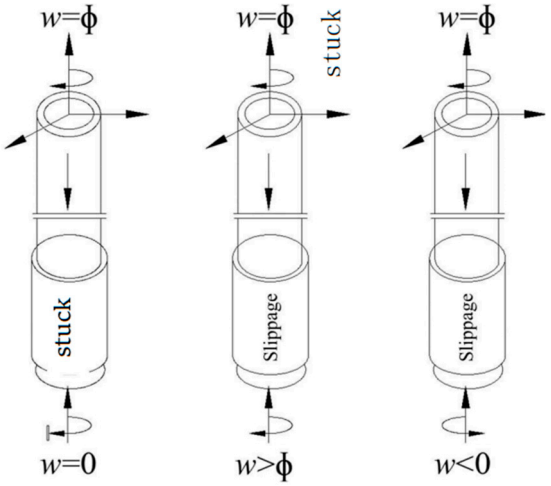

Figure 8. SV diagram of a PDC bit.

Table 4. Basic drill string parameters.

Name	Diameter (in)	Length (mm)	Density (kg/m^3)	Elastic Modulus (Pa)	Poisson's Ratio	Damping Coefficient
Drill String	5″	3000	7900	2.1×10^{11}	0.3125	2

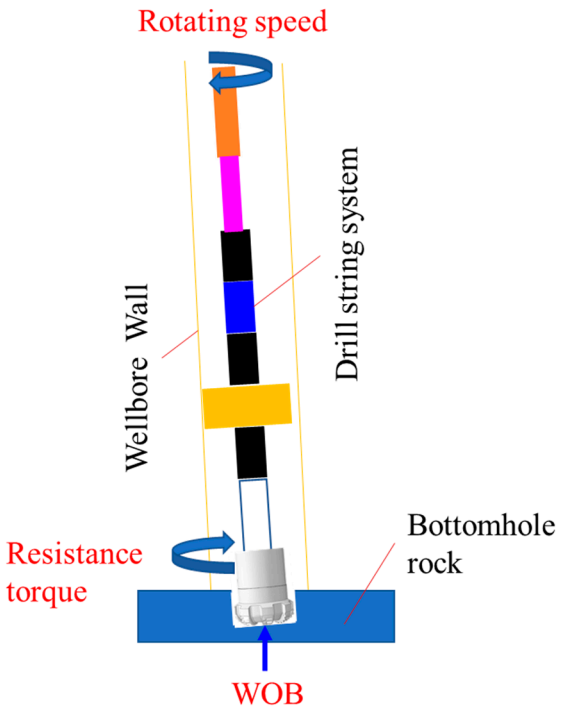

Figure 9. Schematic diagram of drill string system structure.

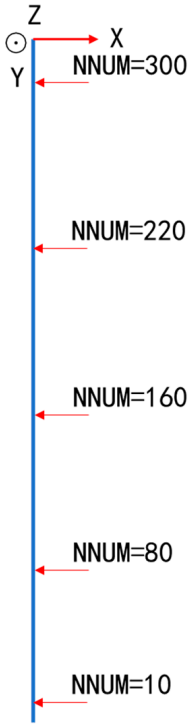

Figure 10. Unit node of the drill string system.

Figure 11. Stress distribution of drill string under static loading.

Figure 12. Torque distribution along dynamic loading drill string.

5.2. Mechanism and Law of SV of the Drill Bit

When the bit rotates under the condition of dynamic balance, the bit resistance suddenly increases, which will lead to the situation of first a decrease and then an increase in the bit's rotational speed. As shown in Figure 13, when the simulation time is 22.1 s, this changes the original arrival time and the stabilization time is 2 s, and then decreases. The bit angular velocity decreasing rapidly from 8.37 rad/s in dynamic equilibrium to 4.2 rad/s indicates the presence of viscosity. Because the speed of the upper rotary table is constant, the drill string distorts and starts to accumulate energy while the drill bit still rotates. When the drill string energy is high enough, the drill bit speed suddenly increases to 13.1 rad/s, and then slippage occurs. Because the drill pipe is an elastic element, the drill bit still rotates at a variable speed after this, and it finally tends towards dynamic balance. Obviously, during the stage of bit slippage, its rotational speed is much higher than that in dynamic balance, which will inevitably cause the cutting teeth to suffer dynamic load impact. With the occurrence of SV, the cutting teeth become prone to premature failure.

Under the same conditions, the torque changes of unit nodes 1, 50, 100, 150, 200, 250, and 300 at different positions of the drill string are shown in Figure 14. When the load changes suddenly, the torque borne by the drill string increases with the depth of the well, and it approaches from the bit to the bit. When dynamic balance is reached, the torque changes from the bottom hole. Therefore, when the drill bit penetration depth changes or the lithology abrupt changes lead to torque, the drill pipe will also bear greater torque, which will lead to SV, and the drill pipe will also bear cyclic variable stress.

Figure 15 shows the rotational speed near the bit when the peak torque is 1.3 times, 1.5 times, 1.7 times and 1.9 times of the initial torque, respectively (corresponding peak torque is 5200 Nm, 6000 Nm, 6800 Nm and 7600 Nm, respectively). When the peak torque applied to the bit exceeds 6500 Nm, obvious viscosity occurs when the bit penetration rate is zero. When the peak torque is 7600 Nm, the rotational speed of the bit is close

to three times that of the dynamic equilibrium, which will easily cause the failure of the cutting teeth, such as the collapse and delamination of the cutting teeth, and then cause the abnormal failure of the bit.

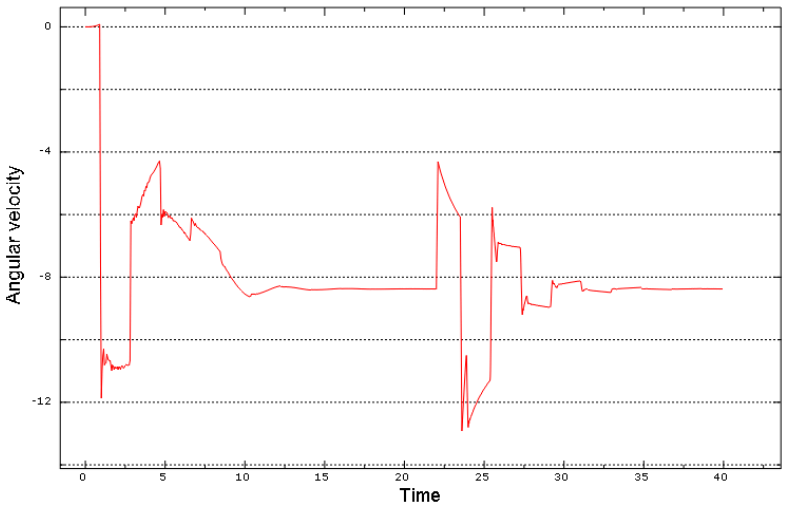

Figure 13. Variation in rotational speed near the bit when the load changes abruptly.

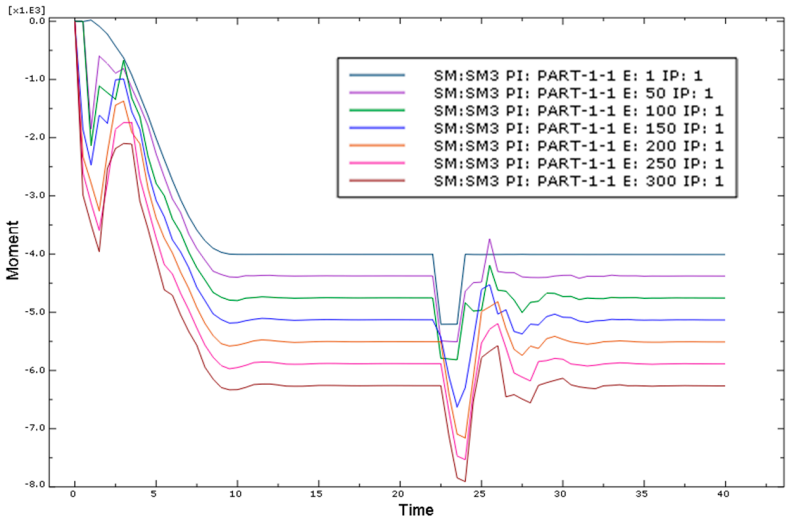

Figure 14. Torque variation at different positions of drill pipe when the load changes abruptly.

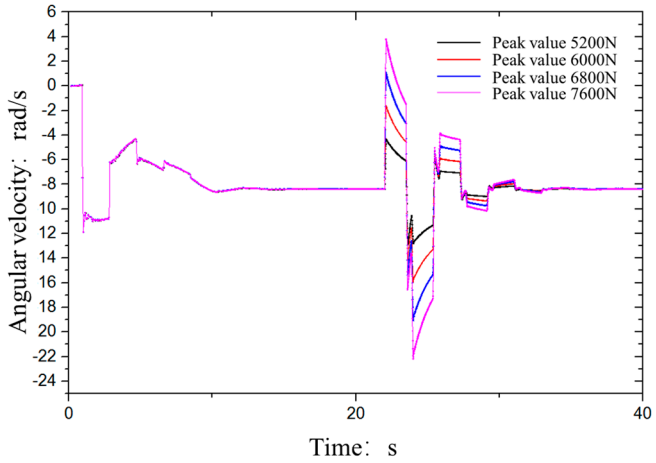

Figure 15. Variation in angular velocity near the bit at different peak torques.

Figure 16 shows the change in bit speed under different drill string lengths. Because the active load (4000 Nm) is applied at the bit, the bit speed fluctuates during the initial stage of drilling. When the drill string is 3000 m, the rigidity of the drill string is sufficient, and the bit does not stop after the initial fluctuation. With this length of the drill string, the rotating speed of the drill bit is far less than the wellhead rotating speed (8.37 rad/s) for a long time. This is the elastic energy storage stage of the drill string. When the drill string reaches 11,000 m, the drill string still stops for a long time after the active load fluctuation (after 5 s), and when the accumulated force of the drill string becomes sufficient, it begins to break. Therefore, even if the bit resistance is constant, the SS phenomenon can occur provided the drill string is long enough.

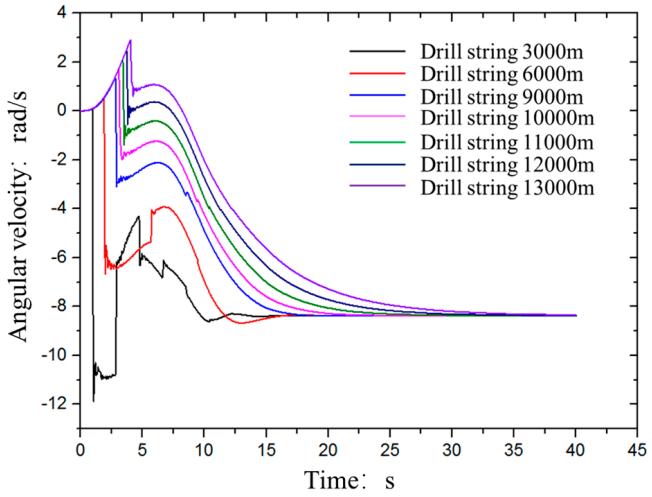

Figure 16. Variation in drilling speed of drill bits under different drill string lengths.

6. Conclusions

(1) The working torque of PDC bit has little influence on parameters such as tooth density and blade number. However, it is greatly affected by the depth of intrusion, strength of the rock, and size of the drill bit. The change in the depth of intrusion (or the sudden change in drilling pressure) has a significant impact on the speed of the drill bit.

(2) The fundamental reason for SV of the bit is that the torque on the bit is insufficient to overcome the resistance of the rock and so the dynamic balance is broken. The main factors affecting SV include the change in stratum rock strength, changes in drill string system length and stiffness, change in the WOB load, and vibration of the drill string system.

(3) When the bit resists torque, the bit speed drops or the bit can even stop running; that is, SS occurs. The drill string distorts and starts to accumulate energy. During the slippage stage, the bit speed is notably higher than the rotary table speed.

(4) When the bit resistance torque is constant, the drill string torque from the bottom hole to the wellhead increases gradually. When the bit reaches a certain critical value, the bit will stop for a long time; that is, SS will occur. When the drill string accumulates enough energy, it will break and reach the dynamic balance again.

(5) To minimize damage to the bit from SV, the following three measures can be taken: 1. The auxiliary cutting structure characteristics of the bit (e.g., the compound cutting structure of backup teeth) can be modified to limit the penetration depth of the cutting teeth within a certain range. 2. The bit structure can be optimized by, for example, using a spiral blade to optimize the transverse unbalanced force of the bit. 3. The drilling parameters can be optimized to control the WOB speed under drilling of heterogeneous formations to prevent the occurrence of SV.

Author Contributions: Conceptualization, L.L.; Methodology, C.Z.; Writing—original draft, A.W. All authors have read and agreed to the published version of the manuscript.

Funding: This research was funded by the Open Fund (PLN2023-33) of National Key Laboratory of Oil and Gas Reservoir Geology and Exploitation (Southwest Petroleum University), Sichuan Provincial Science Foundation Project [2023YFQ0063], and Science Foundation of Yibin University [2019QD19].

Data Availability Statement: Data is contained within the article.

Acknowledgments: Thanks to Southwest Petroleum University for its support of the research.

Conflicts of Interest: The authors declare no conflict of interest.

References

1. Teng, X.Q.; Di, Q.F.; Li, N.; Chen, F.; Zhou, B.; Wang, M. Measurement and Analysis of Stick-Slip Characteristics of Drill String in Ultra-Deep Wells. *Pet. Drill. Tech.* **2017**, *45*, 32–39.
2. Kessai, I.; Benammar, S.; Doghmane, M.Z.; Tee, K.F. Drill Bit Deformations in Rotary Drilling Systems under Large-Amplitude Stick-Slip Vibrations. *Appl. Sci.* **2020**, *10*, 6523. [CrossRef]
3. Laib, A.; Gharib, M. Design of an Intelligent Cascade Control Scheme Using a Hybrid Adaptive Neuro-Fuzzy PID Controller for the Suppression of Drill String Torsional Vibration. *Appl. Sci.* **2024**, *14*, 5225. [CrossRef]
4. Monteiro, H.L.S.; Trindade, M.A. Performance analysis of proportional-integral feedback control for the reduction of stick-slip-induced torsional vibrations in oil well drillstrings. *J. Sound Vib.* **2017**, *398*, 28–38. [CrossRef]
5. Ejike, C.; Obuobi, I.F.; Avinu, S.; Abid, K.; Teodoriu, C. Investigation and Analysis of Influential Parameters in Bottomhole Stick–Slip Calculation during Vertical Drilling Operations. *Energies* **2024**, *17*, 622. [CrossRef]
6. Hosseinzadeh, A.; Bakhtiari-Nejad, F. A New Dynamic Model of Coupled Axial–Torsional Vibration of a Drill String for Investigation on the Length Increment Effect on Stick–Slip Instability. *J. Vib. Acoust.* **2017**, *139*, 061016. [CrossRef]
7. Kovalyshen, Y. Experiments on Stick-Slip Vibrations in Drilling with Drag Bits. In Proceedings of the 48th U.S. Rock Mechanics/Geomechanics Symposium, Minneapolis, MN, USA, 1–4 June 2014.
8. Richard, T.; Detournay, E.; Fear, M.; Miller, B.; Clayton, R.; Matthews, O. Influence of Bit-Rock Interaction on Stick-Slip Vibrations of PDC Bits. In Proceedings of the SPE Annual Technical Conference and Exhibition, San Antonio, TX, USA, 9 September–2 October 2002.
9. Fu, M.; Li, J.H.; Wu, Y.F.; Song, S.B.; Zhao, A.Q.; Li, W.Q. State Feedback and Torque Feed Forward Combined Control System for Suppressing Drill-Strings Stick-Slip Vibration. *J. Northwest. Polytech. Univ.* **2019**, *37*, 291–298. [CrossRef]
10. Kamel, J.M.; Yigit, A.S. Modeling and analysis of stick-slip and bit bounce in oil well drillstrings equipped with drag bits(Article). *J. Sound Vib.* **2014**, *333*, 6885–6899. [CrossRef]
11. Li, F. Effect of depth-of-cut control (DOC) of PDC bits on stick-slip suppression and rate of penetration improvement. *Pet. Drill. Prod. Technol.* **2021**, *43*, 566–573.
12. Abdul-Rani, A.M.; Ibrahim, K.; Ab Adzis, A.H.; Maulianda, B.T.; Mat Asri, M.N. Investigation on the effect of changing rotary speed and weight bit on PCD cutter wear. *Pet. Explor. Prod. Technol.* **2019**, *10*, 1–6. [CrossRef]
13. Tian, J.L.; Liu, Y.D.; Xiong, J. Research on Stick-slip Vibration Characteristics of Drill String with Longitudinal-torsion Coupling. *Mech. Sci. Technol.* **2022**, *41*, 511–516.
14. MacLean, J.D.; Vaziri, V.; Aphale, S.S.; Wiercigroch, M. Suppressing stick–slip oscillations in drill-strings by Modified Integral Resonant Control. *Int. J. Mech. Sci.* **2022**, *228*, 107425. [CrossRef]
15. Mohammad, J.M.; Clóvis, D.A.M.; Hodjat, S. Nonlinear integrated dynamic analysis of drill strings under stick-slip vibration. *Appl. Ocean Res.* **2021**, *108*, 102521.
16. Derbal, M.; Gharib, M.; Refaat, S.S.; Palazzolo, A.; Sassi, S. Fractional-order controllers for stick-slip vibration mitigation in oil well drill-strings. *J. Low Freq. Noise Vib. Act. Control* **2021**, *40*, 1571–1584. [CrossRef]
17. Fu, M.; Li, J.B.; Wu, Y.F.; Li, Y.R. Characteristic Simulation and Mechanisms Analysis for Drill—Strings Stick-Slip Vibration. *J. Northwest. Polytech. Univ.* **2016**, *34*, 467–472.
18. Vaziri, V.; Kapitaniak, M.; Wiercigroch, M. Suppression of drill-string stick–slip vibration by sliding mode control: Numerical and experimental studies. *Eur. J. Appl. Math.* **2018**, *29*, 805–825. [CrossRef]
19. Cruz Neto, H.J.; Trindade, M.A. Control of drill string torsional vibrations using optimal static output feedback. *Control Eng. Pract.* **2023**, *130*, 105366. [CrossRef]
20. Ulf, J.F.A.; Nathan, V.D.W. Axial and torsional self-excited vibrations of a distributed drill-string. *J. Sound Vib.* **2019**, *444*, 127–151.
21. Bi Siyi, Y. PDC Bit Self-adjusting Depth-of-cut Control Technology. *Pet. Mach.* **2017**, *45*, 40–45.
22. Selnes, K.S.; Clemmensen, C.; Nils, R. Drilling Difficult Formations Efficiently With the Use of an Antistall Tool. *SPE Drill. Complet.* **2009**, *24*, 531–536. [CrossRef]
23. Bakhtiari-Nejad, F.; Hosseinzadeh, A. Nonlinear dynamic stability analysis of the coupled axial-torsional motion of the rotary drilling considering the effect of axial rigid-body dynamics. *Int. J. Non-Linear Mech.* **2017**, *88*, 85–96. [CrossRef]

24. Chen, S.L.; Wisinger, J.; Dunbar, B.; Chris, P. Identification and Mitigation of Friction- and Cutting-Action-Induced Stick/Slip Vibrations with PDC Bits. *SPE Drill. Complet.* **2020**, *35*, 576–587. [CrossRef]
25. Thomas, R.; Christophe, G.; Emmanuel, D. A simplified model to explore the root cause of stick–slip vibrations in drilling systems with drag bits. *J. Sound Vib.* **2007**, *305*, 432–456.
26. Boukredera, F.S.; Hadjadj, A.; Youcefi, M.R. Drill String Torsional Vibrations Modeling With Dynamic Drill Pipe Properties Measurement and Field Validation. *J. Energy Resour. Technol. Trans. ASME* **2022**, *144*, 024502. [CrossRef]
27. Pauline, M.N.; Adrian, A.; Ulf, J.F.A.; Ole, M.A. Evaluation of distributed damping subs with active control for stick-slip reduction in drilling. *Geoenergy Sci. Eng.* **2023**, *231*, 212255.
28. Lobo, D.M.; Ritto, T.G.; Castello, D.A. A novel stochastic process to model the variation of rock strength in bit-rock interaction for the analysis of drill-string vibration. *Mech. Syst. Signal Process.* **2020**, *141*, 106451. [CrossRef]
29. Caresta, M. Drill string Torsional Vibrations Cancelation during Off-Bottom Operations. *SPE Drill Complet.* **2022**, *37*, 141–150.
30. Kapitaniak, M.; Vaziri, V.; Páez, C.J.; Wiercigroch, M. Experimental studies of forward and backward whirls of drill-string. *Mech. Syst. Signal Process.* **2018**, *100*, 454–465. [CrossRef]
31. Guo, X.Q.; Liu, J.; Wang, J.X.; Li, X.; Wei, A.C.; Zhu, H.Y. Study on Axial-lateral-torsion Coupling Vibration Model and Stick-slip Characteristics of Drilling String in Ultra-HPHT Curved Wells. *J. Mech. Eng.* **2022**, *58*, 119–135.
32. Real, F.F.; Batou, A.; Ritto, T.G.; Desceliers, C.; Aguiar, R.R. Hysteretic bit/rock interaction model to analyze the torsional dynamics of a drill string. *Mech. Syst. Signal Process.* **2018**, *111*, 222–233. [CrossRef]
33. Richard, T.; Germay, C.; Detournay, E. Self-excited stick–slip oscillations of drill bits. *Comptes Rendus Mec.* **2004**, *332*, 619–626. [CrossRef]
34. Besselink, B.; Wouw, Y.D.N.; Nijmeijer, H. A semi-analytical study of stick-slip oscillations in drilling systems. *J. Comput. Nonlinear Dyn.* **2011**, *6*, 021006. [CrossRef]
35. Silveira, M.; Wiercigroch, M. Low dimensional models for stick-slip vibration of drill-strings (Conference Paper). *J. Phys. Conf. Ser.* **2009**, *181*, 012056. [CrossRef]
36. Mendil, C.; Kidouche, M.; Doghmane, M.Z.; Benammar, S.; Tee, K.F. Rock–bit interaction effects on high-frequency stick-slip vibration severity in rotary drilling systems. *Multidiscip. Model. Mater. Struct.* **2021**, *17*, 1007–1023. [CrossRef]
37. Jain, J.R.; Ledgerwood, L.W.; Olivier, J.H.; Thorsten, S.; Danielle, M.F. Mitigation of Torsional Stick-Slip Vibrations in Oil Well Drilling through PDC Bit Design: Putting Theories to the Test. In Proceedings of the SPE Annual Technical Conference and Exhibition, Denver, CO, USA, 23–25 October 2011.
38. Yang, H.L.; Yang, Y.L.; Huang, Y.X.; Zhang, H.J.; Liang, L.X. Development and Optimization of a High-Frequency Axial-Torsional Composite Percussion Drilling Tool for Enhanced Impact Technology. *SPE J.* **2024**, *29*, 860–875. [CrossRef]
39. Thorsten, S.; Lance, E.; Jayesh, R.J.; Hatem, O.; Danielle, M.F.; Leroy, W.L. Development and Testing of Stick/Slip-Resistant PDC Bits. In Proceedings of the IADC/SPE Drilling Conference and Exhibition, Fort Worth, TX, USA, 4–6 March 2014.
40. Hareland, G.; Nygaard, R.; Yan, W.; Wise, J.L. Cutting Efficiency of a Single PDC Cutter on Hard Rock. *J. Can. Pet. Technol.* **2009**, *48*, 60–65. [CrossRef]
41. *SY/T 5561-2014*; Drill Pipe. National Energy Administration: Beijing, China, 2014.